



Interactions between nano-TiO₂ and the oral cavity: Impact of nanomaterial surface hydrophilicity/hydrophobicity



Birgit J. Teubl^a, Christa Schimpel^a, Gerd Leitinger^{b,c,d}, Bettina Bauer^a,
Eleonore Fröhlich^{c,d}, Andreas Zimmer^{a,d}, Eva Roblegg^{a,d,*}

^a Institute of Pharmaceutical Sciences, Department of Pharmaceutical Technology, University of Graz, 8010, Austria

^b Institute of Cell Biology, Histology and Embryology, Research Unit Electron Microscopic Techniques, Medical University of Graz, 8010, Austria

^c Center for Medical Research, Medical University of Graz, 8010, Austria

^d BioTechMed, Graz 8010, Austria

HIGHLIGHTS

- Hydrophilic as well as hydrophobic TiO₂ NPs agglomerated under oral physiological conditions.
- Particles penetrated the upper and lower buccal epithelium, independent on the degree of hydrophilicity.
- Most of the hydrophobic particles were found in vesicular structures, while hydrophilic particles were freely distributed in the cytoplasm.
- Hydrophilic particles had a higher potential to trigger toxic effects (e.g., ROS) than hydrophobic particles.

ARTICLE INFO

Article history:

Received 10 October 2014

Received in revised form

16 December 2014

Accepted 30 December 2014

Available online 5 January 2015

Keywords:

Titanium dioxide nanoparticles

Hydrophilicity/hydrophobicity

Oral cavity

Intracellular distribution

Toxicity

ABSTRACT

Titanium dioxide (TiO₂) nanoparticles are available in a variety of oral applications, such as food additives and cosmetic products. Thus, questions about their potential impact on the oro-gastrointestinal route rise. The oral cavity represents the first portal of entry and is known to rapidly interact with nanoparticles. Surface charge and size contribute actively to the particle–cell interactions, but the influence of surface hydrophilicity/hydrophobicity has never been shown before. This study addresses the biological impact of hydrophilic (NM 103, rutile, 20 nm) and hydrophobic (NM 104, rutile, 20 nm) TiO₂ particles within the buccal mucosa. Particle characterization was addressed with dynamic light scattering and laser diffraction. Despite a high agglomeration tendency, 10% of the particles/agglomerates were present in the nanosized range and penetrated into the mucosa, independent of the surface properties. However, significant differences were observed in intracellular particle localization. NM 104 particles were found freely distributed in the cytoplasm, whereas their hydrophobic counterparts were engulfed in vesicular structures. Although cell viability/membrane integrity was not affected negatively, screening assays demonstrated that NM 104 particles showed a higher potential to decrease the physiological mitochondrial membrane potential than NM 103, resulting in a pronounced generation of reactive oxygen species.

© 2015 Elsevier B.V. All rights reserved.

1. Introduction

The number of new generations of nanomaterials associated with new perspectives on material physics is steadily increasing. Titanium dioxide (TiO₂) (nano) particles (NPs), for example, are manufactured worldwide in large quantities [1] and are used in a variety of oral applications (such as sugar-films, toothpaste, sun-

screen lotions or tablets/capsules) [2]. Thus, humans are constantly exposed to TiO₂ NPs, which makes the oro-gastro-intestinal uptake route important for risk assessment studies [3].

Once particles are taken orally—whether intended or unintended—they get in contact with the oral cavity, which represents the first delivery portal for the oral uptake route [4]. From an anatomical point of view it comprises a stratified squamous epithelium, which is covered by a mucus layer. This layer is formed by high-molecular-weight mucopolysaccharides (also referred to as mucins), which are components of the saliva and adhere onto the superficial cells to prevent uncontrolled uptake of foreign substances. Previous studies demonstrated that NPs rapidly

* Corresponding author at: Institute of Pharmaceutical Sciences, Department of Pharmaceutical Technology, University of Graz, Universitätsplatz 1, A-8010, Graz, Austria. Tel.: +43 316 380 8888; fax.: +43 316 380 9100.

E-mail address: eva.roblegg@uni-graz.at (E. Roblegg).

interact with the mucus layer, penetrate the underlying tissue within a few minutes and impact the physiological homeostasis of buccal/sublingual cells in the oral cavity [5–7].

However, the reactivity of TiO₂ NPs is dependent on their physicochemical properties, such as size, surface charge and crystallinity (i.e., anatase, rutile or brookite) [8,9]. Specifically for cosmetics, there is a further key parameter that has to be considered. TiO₂ particles are often coated with organic (e.g., silane) or inorganic (e.g., alumina, silica) materials to enhance the compatibility with lipophilic components of cosmetic applications. As a consequence, the particle's surface hydrophilicity/hydrophobicity is altered [10,11] and the biological reactivity, the penetration depth and the intracellular particle distribution are expected to change [5,6]. Regarding the uptake efficiency in the gastrointestinal tract it is known that hydrophilic surfaces cause a decreased uptake rate compared to more hydrophobic ones [12]. Studies performed by Qiao et al. demonstrated that hydrophobic fullerene NPs penetrated the membrane after they were embedded in the inner phase of the lipid bilayer [13]. A different response mechanism was described for the hydrophilic derivatives, which were only adsorbed onto the bilayer. This phenomenon was confirmed by Li et al. who demonstrated via computational simulation that hydrophilic NPs favor adsorption on the surface rather than inclusion into the bilayer [14]. Thus, the membrane wrapping process is impeded, nanoparticles enter the cells via energy-independent pathways and are freely distributed in the cytoplasm [15,16]. This is often linked to the generation of reactive oxygen (ROS) and nitrogen species, resulting in inflammation and/or cell death [17,18]. Although TiO₂ is not considered as a hazardous material under standard human exposure conditions, this phenomenon is also reported for TiO₂ NPs [19]. Further consequences are seen in harmful DNA alterations and mutagenic/genotoxic effects due to direct or indirect interference with the structure and function of genomic DNA [20–26]. If particles closely interact with the cell membrane, they are internalized via endocytic mechanisms (i.e., phagocytosis, macropinocytosis, clathrin-mediated endocytosis, caveolae-mediated endocytosis and clathrin/caveolae-independent endocytosis), enclosed within vesicular structures and separated from the cytoplasm. Thus, they do not get in contact with the cytosol or with organelles and are considered as less toxic [27].

To our knowledge the impact of TiO₂ NPs on penetration, intracellular distribution and cytotoxicity with respect to hydrophilicity/hydrophobicity in the oral cavity has not been investigated yet. In this study – to learn more about the relationship between buccal mucosa and TiO₂ NPs—two distinct reference particles listed by the Organization for Economic Co-operation and Development (OECD) with the same crystallinity (i.e., rutile) and the same nominal size (20 nm) were used, on the one hand coated with a hydrophobic substance (NM 103) and on the other hand with a hydrophilic one (NM 104). Physicochemical properties of TiO₂ particles in different (biological) media were carefully studied with dynamic light scattering (DLS) and laser diffraction (LD). Surface hydrophilicity/hydrophobicity was determined with the Rose Bengal (RB) adsorption method. Penetration/permeation studies of nano-TiO₂ into excised porcine mucosa were performed using Franz diffusion cells. NP localization was examined with transmission electron microscopy (TEM) and the detected particles were identified via energy filtered TEM (EFTEM). To gain insights into the intracellular particle distribution of TiO₂ particles, co-localization studies of fluorescently labeled TiO₂ particles (Alizarin Red S) with lysosomes/mitochondria were conducted with a human buccal cell line (TR146), using Confocal laser scanning microscopy (LSM). Furthermore, potential (cyto-/geno-) toxic effects were examined using 3-(4,5-dimethylthiazol-2-yl)-5-(3-carboxymethoxyphenyl)-

2-(4-sulfophenyl)-2H-tetrazolium) (MTS), lactate dehydrogenase (LDH), dihydroethidium (DHE), tetramethylrhodamin methyl ester (TMRM) and hypoxanthine-guanine phosphoribosyl transferase (HPRT)-forward-mutation assays.

2. Materials and methods

Particles were kindly provided by the OECD. Hydrophobic (NM 103, rutile, 20 nm, dimethicone coated) and hydrophilic TiO₂ particles (NM 104, rutile, 20 nm, glycerol coated) were manufactured by Sachtleben, Duisburg, Germany. Substances used for TEM sample preparation, the dye Rose Bengal and porcine mucin were supplied by Sigma–Aldrich, Vienna, Austria. Materials used for cell culture experiments were provided by Invitrogen as not otherwise stated.

2.1. Particle characterization

The mean ferret diameter of primary particle sizes was calculated out of ten TEM images using the software ImageJ. physicochemical properties of TiO₂ particles were characterized in physiological relevant media i.e., phosphate buffered saline (PBS) and artificial saliva [5]. To obtain de-agglomerated TiO₂ particles, the dispersions (0.4 mg/mL) were ultra-sonicated as previously described [7] and measured with Zetasizer Nano SP (Malvern Instruments, Malvern, UK) by the use of DLS. The potential impact of ultrasonication to the chemical morphology of TiO₂ particles were precluded by means of Fourier transform infrared spectroscopic measurements (FTIR). Additional size analysis was conducted by LD (Malvern Instruments, Malvern, UK) using the Mie theory. The refractive indices (RI) of the measuring media were 1.33 for PBS and water and 1.334 for artificial saliva. The real RI for the investigated particles was 2.874 and the imaginary RI was 0.01. The results of the particle diameters are presented as *d*(0.1), *d*(0.5) and *d*(0.9), which means that 10%, 50% or 90% (number distribution) of the measured particles are below the given size (*n* = 3).

The degree of surface hydrophobicity/hydrophilicity was determined with the RB adsorption method, where the adsorption of the hydrophobic dye RB onto the particle surface was measured [28]. TiO₂ particles were dispersed in a graded series of RB/PBS solution (10–50 µg/mL) for 3 h at room temperature and centrifuged for 3 h at 20,817 × *g*. The supernatant was measured spectrophotometrically at 544 nm (FLUOstar Optima, BMG Labortechnik) and binding constants (*K*) of the RB dye were calculated as previously described [28].

2.2. Ex-vivo permeability studies

The ex-vivo permeability studies of TiO₂ particles were performed with porcine buccal mucosa, which has been considered as best suited model that mimics the human mucosa due to morphological and enzymatic similarities [20]. The tissue was obtained from freshly sacrificed pigs (age: <6 months; Karnerta Slaughter House, Graz, Austria) and transported in 4°C Krebs buffer. The tissue was trimmed to achieve uniform thickness (500–800 µm) and to remove the underlying tissue. The maintenance of viability and integrity of the tissue during the experiment was examined as previously described [5]. Ex-vivo studies were conducted with static Franz diffusion cells (PermeGear, USA, 11.28 mm jacketed cell) (*n* = 6). The receiver compartment of the diffusion chamber was filled with 8 mL pre-warmed PBS buffer and physiological temperature of 37 ± 0.5 °C was assured by a surrounded water jacket. The excised buccal mucosa was mounted within the diffusion cells, so that the epithelium faced the donor and the connective tissue region faced the receiver compartment. After 30 min equilibration time with pre-warmed PBS buffer, 1 mL TiO₂/PBS dispersion (100 µg/mL) was applied and incubated for 4 h. The mucosa was

washed 3 times with PBS and further treated for the used visualization method.

2.3. Transmission electron microscopy (TEM)/energy filtered transmission microscopy (EFTEM)

The tissue was fixed after ex-vivo studies with 2% paraformaldehyde/2.5% glutaraldehyde for 5 h and placed into 0.1 M sodium cacodylate buffer overnight (4 °C). Subsequently, post-fixation was carried out in 1.0% osmium tetroxide and dehydration was performed through a graded series of ethanol (50–100%). The tissue samples were treated with propylene oxide and embedded into epoxy resin. Thin sections were obtained from the upper and lower epithelium and placed onto 300 mesh copper grids. Grids were stained using lead citrate and uranyl acetate. Images were acquired using a TEM model FEI-Tecnai-20 equipped with a GATAN quantum GIF (model 963) energy filter. The analyzed test fields ($n = 12$) were chosen randomly within the upper and lower mucosa and considered as representative when at least 9 of the analyzed fields included verified TiO₂ particles.

Elemental maps were conducted in regions of interest with a three-window method and a slit width of 30 eV. Two windows used for calculating the background were placed in front of the L_{2,3} edge of titanium at 435 eV, the third window was placed past this edge.

2.4. Co-localization studies of TiO₂ with lysosomes/mitochondria

For co-localization studies of particles with lysosomes/mitochondria, 4×10^4 cells/200 μ L medium were seeded in WillCo Dishes[®] (WillCo Wells BV, Amsterdam, Netherlands; growth area: 1.13 cm²) and incubated for 24 h under standard conditions at 37 °C. Subsequently, the cells were washed twice with 200 μ L PBS and incubated with 100 μ g/mL of the respective TiO₂/PBS dispersion for 4 h. Prior to experiments, particles were labeled with Alizarin Red S as described elsewhere [29]. To visualize mitochondria, cells were incubated with MitoTracker DeepRed 633 (Invitrogen) (200 nM) for 20 min at 37 °C. Lysosomes were stained by incubation with Lyso Tracker Green DND-26 (Invitrogen) (50 nM) for 5 min at 37 °C. Afterwards, cells were washed twice and images were taken with a LSM510 Meta confocal laser scanning microscope (Zeiss) with 488/BP 505–550 (Lyso Tracker Green DND 26) or 633/BP 679–754 nm (MitoTracker DeepRed 633) for the green channel and 543/LP 560 for the red channel (Alizarin Red S coated TiO₂).

2.5. Cell viability/membrane integrity

Human buccal epithelial TR146 cells were achieved from Imperial Cancer Research Technology (London, UK). Cell cultivation was performed as described previously [30,31]. 2×10^4 cells/200 μ L medium cells were seeded in 96 well plates and incubated for 24 h ($n = 2$). Thereafter, the medium was exchanged by different concentrated TiO₂ particles/PBS dispersion (i.e., 1–200 μ g/mL, 6 replicates) and incubated for 4 h. MTS assay was performed with a CellTiter 96[®] Aqueous Non-Radioactive Cell Proliferation Assay (Promega). 20 μ L of a MTS/5-methyl-phenazinium methyl sulfate (PMS) solution per well were supplemented and the absorbance was measured after 4 h incubation time at 490 nm with a VIS-plate reader (FLUOstar Optima, BMG, Labortechnik). The membrane integrity was assessed using a CytoTox-ONE[™] Homogeneous Membrane Integrity Assay (Promega) ($n = 2$). The positive control was treated with 2 μ L of lysis solution (6 replica) and assumed as 100% release of LDH. 25 μ L of the supernatant were mixed with 25 μ L of the CytoTox-ONE Reagent and incubated for 20 min at 37 °C and for further 10 min at RT. The LDH release was recorded after the

reaction was stopped (12.5 μ L stop solution) with fluorimeter (FLUOstar Optima, BMG, Labortechnik) at 560 nm excitation wavelength and 590 nm emission wavelength.

2.6. Generation of reactive oxidative stress (ROS)/alterations in mitochondrial membrane potential

Generation of ROS was assessed by the ROS-driven conversion of non-fluorescent DHE to fluorescent ethidium. 2×10^4 cells were seeded in 96 well plates and incubated for 24 h. Subsequently, cells were treated with 100 μ g/mL TiO₂/PBS dispersions, 200 μ M H₂O₂ (positive control) or PBS (negative control), respectively ($n = 2$, 6 replicates) and 10 μ M DHE was added. After 4 h incubation time, the generation of ROS was measured with a fluorimeter at 544 nm excitation and 612 nm emission. TMRM was used to evaluate temporal changes in the mitochondrial membrane potential. When the membrane potential is disturbed due to different influencing factors, the cationic dye accumulates in the mitochondria, which results in diminished fluorescence due to self-quenching. Different concentrations of TiO₂ particles/HBSS medium dispersion (i.e., 1–200 μ g/mL, 6 replicates) were applied as well as positive (H₂O₂) and negative (HBSS) controls and incubated for 4 h. Subsequently, cells were washed twice with 200 μ L Hank's Balanced Salt Solution (HBSS) and 1 μ M TMRM/HBSS solution was applied and incubated for 20 min at 37 °C. Afterwards, cells were washed again and analyzed at 590 nm excitation wavelength and 612 nm emission wavelength.

2.7. Hypoxanthine-guanine phosphoribosyl transferase (HPRT)-gene-mutation-assay

The HPRT assay is an in vitro mammalian cell gene mutation test. This test system is appropriate for use in the initial assessment of the genotoxicity of TiO₂ particles (OECD guideline 476). The assay was performed with a V79 Chinese hamster cell line. These cells only have one functional copy of the gene which codes for the HPRT enzyme. HPRT enzyme activity is important for DNA synthesis. The use of the toxic nucleoside analog 6-thioguanine forms the basis for cell selection following treatment. Cells without a mutation are poisoned by 6-thioguanine, while mutant cells survive and form colonies. Those cells that are able to form colonies are assumed to be mutant cells resulting from induced mutation caused by TiO₂. As indication for colony formation formazan bioreduction was performed [32].

V79 cells were cultivated in RPMI medium supplemented with 10% fetal bovine serum (FBS), 1% L-glutamine and 1% penicillin/streptomycin. Cells were maintained in a humidified incubator at 37 °C with 5% CO₂. For the experiment, 6 million cells were seeded into flasks and were treated with NM103 and NM104 TiO₂ particles (100 μ g/mL) for 4 h. 50 μ g/mL N-Nitroso-N-ethylurea (ENU, Sigma-Aldrich) was used as positive control. Subsequently, the cells were rinsed in DMEM + 10% FBS and cultured for additional 24 h. Thereafter, cells were removed by trypsin/EDTA treatment and re-seeded at a cell density of 1×10^6 /flask in the same medium. An aliquot of these cells was cultured for 7 days in DMEM + 10% FBS to determine plating efficacy. After 4 days, the cells were sub-cultured and transferred to the selection medium (DMEM containing 10 μ g/mL 6-thioguanine and 5% FBS). Again an aliquot of these cells was cultured for 7 days in DMEM + 10% FBS to determine plating efficacy. Medium was changed every 3 days. After 9 days in culture, the amount of surviving cells was determined. Since the pilot experiments showed that, similar to the data by Buch et al. [32], the number of colonies was linearly correlated to absorbance in the MTS assay, this read-out was used for the assessment.

Table 1
DLS measurements of hydrodynamic diameter (nm) and surface charge (ζ -potential) of TiO₂ particles in different (biological) dispersants.

PBS	<i>d</i> (nm)	ζ (mV)	PdI
NM 103	1819 ± 61.56	-25.2 ± 8.2	0.133 ± 0.082
NM 104	1539 ± 489	-21.1 ± 4.3	0.236 ± 0.087
Artificial saliva	<i>d</i> (nm)	ζ (mV)	PdI
NM 103	3061 ± 134.4	-9.5 ± 3.7	0.269 ± 0.028
NM 104	2597 ± 426	-9.1 ± 3.3	0.236 ± 0.087

3. Results and discussion

3.1. Particle characterization

Particle characterization was performed under physiological conditions simulating the environment in the oral cavity (i.e., ionic strength, proteins and pH). First, the degree of hydrophobicity/hydrophilicity was estimated with the RB adsorption method, which allows direct quantification of the relative particle surface hydrophobicity in the dispersion medium. The amount of the hydrophobic dye bound onto the particle surface is determined and the calculated binding constant (mL/mg) is stated as degree of hydrophilicity/hydrophobicity. RB constants showed that NM 103 exhibited a slightly hydrophobic surface (0.09 mL/mg), while the surface of NM 104 was hydrophilic (0.04 mL/mg). The primary particle size, which is thought to be a significant trait that controls particle uptake and intracellular localization, was determined with TEM. The results revealed sizes from 28 nm to 49 nm, independent on the material's nature. Thus, conclusions of particle interactions were exclusively drawn on the surface hydrophobicity/hydrophilicity.

The dispersion status of particles was observed by the use of DLS, using two distinct media. As expected, a high agglomeration tendency was observed in PBS (mimicking the pH and the ionic content of saliva), presumably due to the high concentration of ions, resulting in a decreased electrical double-layer repulsive energy between the particles (Table 1) [33]. Additionally, the particle behavior was investigated in artificial saliva since mucins play a major role in the oral environment. The results demonstrated that TiO₂ particles significantly agglomerated/increased in size independent of the surface properties (Table 1). This is due to the high ionic strength and the contained mucins in saliva. Cell-associated mucins, for example, show sizes from 100 to 500 nm (cell-associated mucins) and secreted mucins are about several microns in size [34–36]. Thus, the effect of size enlargement can be attributed to agglomeration and additionally, to the interactions between particles and the negatively charged mucins.

Furthermore, LD was used as a complementary particle characterization technique. It was demonstrated that hydrophilic and hydrophobic TiO₂ were highly polydisperse in all investigated media and the majority of the particles was present in the micro-sized range (Table 2). Overall, there was a good correlation between the *d*₉₀ values of LD and the results of DLS. However, LD measurements provided deeper insights into the particle dispersion state,

Table 2
LD measurements of hydrodynamic diameter (nm) of TiO₂ particles in different (biological) dispersants.

PBS	<i>d</i> (0.1)	<i>d</i> (0.5)	<i>d</i> (0.9)
NM 103	445.67 ± 1.15	722.67 ± 11.24	1535.33 ± 45.72
NM 104	502.67 ± 2.52	734.33 ± 4.04	1364.33 ± 10.02
Artificial saliva	<i>d</i> (0.1)	<i>d</i> (0.5)	<i>d</i> (0.9)
NM 103	746.00 ± 18.52	1344.00 ± 38.94	2383.33 ± 62.29
NM 104	588.67 ± 1.5	1215.33 ± 10.02	3039.67 ± 142.20

since a significant amount (10%) of nano-sized particles was present despite high particle agglomeration. These results imply that in physiological fluids such as saliva, 10% of the exposed NP amount shows the appropriate size to interact with cells in the oral cavity [7]. Notably, no marked influence of hydrophilicity or hydrophobicity on the polydispersity/dispersion state of the nano-samples was observed.

3.2. Penetration/permeation of TiO₂ particles into/through the buccal mucosa and co-localization with lysosomes

Ex-vivo experiments with fresh porcine buccal epithelium were performed to evaluate whether there is a difference in penetration/permeation behavior between hydrophilic and hydrophobic TiO₂ particles. Generally, the buccal mucosa comprises a stratified squamous epithelium (upper part), which is covered with a mucus layer, followed by the basal lamina and the connective tissue (lower part). The investigations with TEM (Figs. 1 and 2A–D) and EFTEM (Figs. 1 and 2E–H) demonstrated that both TiO₂ particles permeated the first buccal barrier (i.e., the mucus layer) and penetrated into the epithelium. NM 103 and NM 104 were located in the upper parts and in the lower parts (Figs. 1 and 2). These data suggest that the penetration/permeation behavior of TiO₂ NPs in the oral cavity is not significantly influenced by the hydrophilicity/hydrophobicity. However, the hydrophobic NM 103 particles were found closely aligned to the cell membrane (Fig. 1B and F) and engulfed in vesicular structures (Fig. 1A, C, E, G). This strongly suggests that the hydrophobic particle surface-coating leads to nonspecific binding forces with the buccal cell membrane and promotes cellular uptake. More precisely, it seems that adsorptive endocytosis is involved, which is in accordance with studies by Verma et al. [37,38]. A minor extent of NM 103 particles was also found non-membrane-bound within the cytoplasm (Fig. 1D and H). This observation can be explained due to the different stages during endosomal uptake. The ingested particles are usually transported via endosomes and late endocytic particles to lysosomes [39]. Since metaloxide NPs are not biodegradable, lysosomes can release TiO₂ unaltered into the cytoplasm. In contrast, hydrophilic NM 104 particles were exclusively found freely distributed in the cytoplasm (Fig. 2A–H). This phenomenon is consistent with studies reported by Geiser et al. [40]. They observed that NP uptake into red blood cells did not occur via endocytosis, but via passive pathways, such as diffusion through pores. Previous studies performed by our group also showed that hydrophilic anatase TiO₂ particles [7] were internalized by the cells within 10 min and most of them were located in the cytoplasm. Thus, direct penetration of the buccal surface membrane without the need of endocytic mechanisms is likely to occur due to nonspecific binding forces [41]. This may lead to the formation of transient holes in the plasma membrane, which might affect the membrane integrity/potential [42]. The membrane integrity was assessed by measuring the LDH release. Since LDH assays demonstrated that the membrane integrity was not significantly affected (<10% for all tested NP concentrations), we assume that TiO₂ particles are capable of penetrating membranes without causing membrane poration.

To verify this hypothesis, co-localization studies were performed. TiO₂ NPs were fluorescently labeled with Alizarin Red S and lysosomes were identified by Lyso-Tracker. Cells were incubated for 4 h and recorded with LSM. Regarding the lysosomal uptake, Fig. 3 demonstrates that hydrophobic NM 103 particles mostly accumulated within lysosomes (yellow co-localization), whereas the hydrophilic NM 104 particles were still located at the lysosomal periphery. This observation further supports the assumption that NM 103 particles are taken up via endocytosis and transported via vesicular structures to form endosomes that later on fuse with lysosomes [43,44]. However, the fact that NM 104 particles were

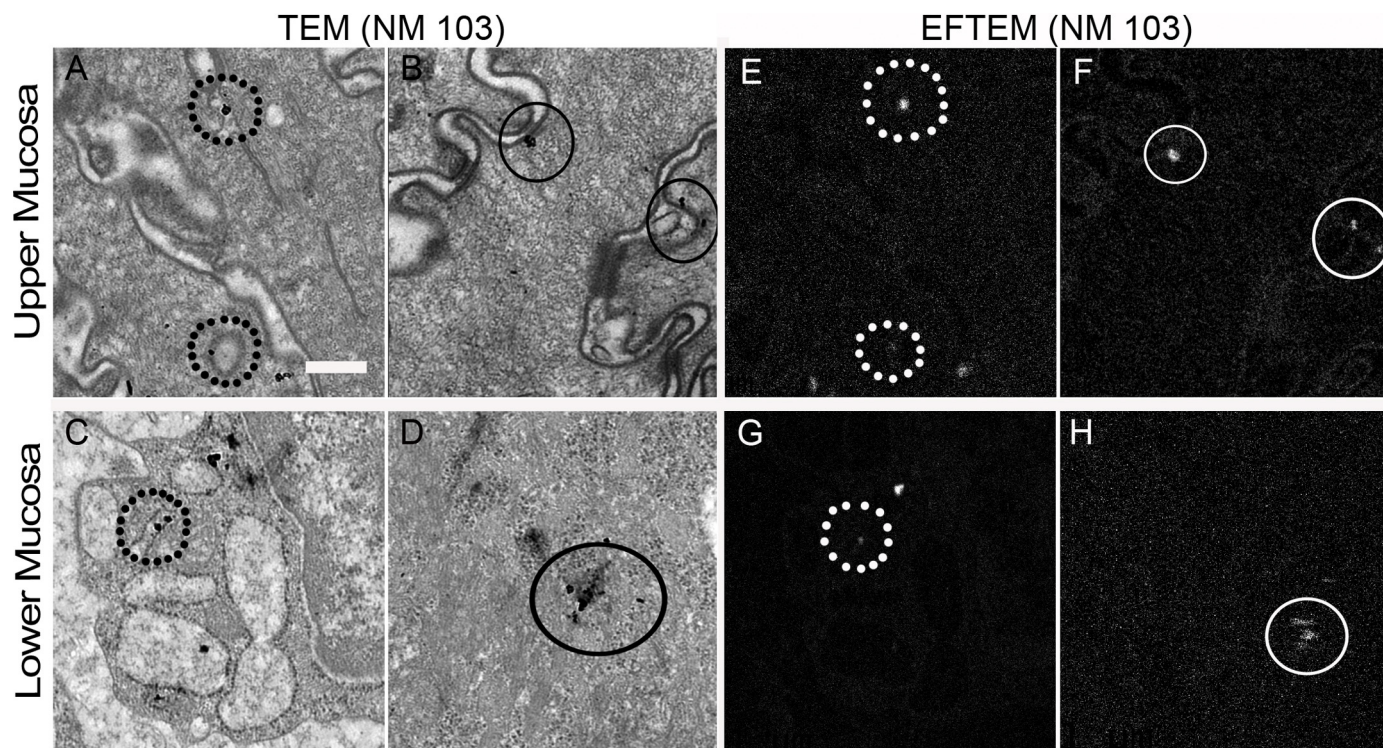


Fig. 1. TEM images of the buccal mucosa (cross sections) after 4 h particle incubation. NM 103 particles were found in the upper mucosa (superficial epithelium; upper panel) and in the lower mucosa (basal lamina/ connective tissue; lower panel). NM 103 particles were located in vesicular structures (A, C, dotted circles), closely aligned to the cellular membrane (B, circles) and a minor extent was found freely distributed in the cytoplasm (D, circles). To verify the particles of interest, EFTEM was performed and elemental maps were made with a three-window method (E–H). The maps verified the element titanium (white spots). (Scale bar = 500 nm).

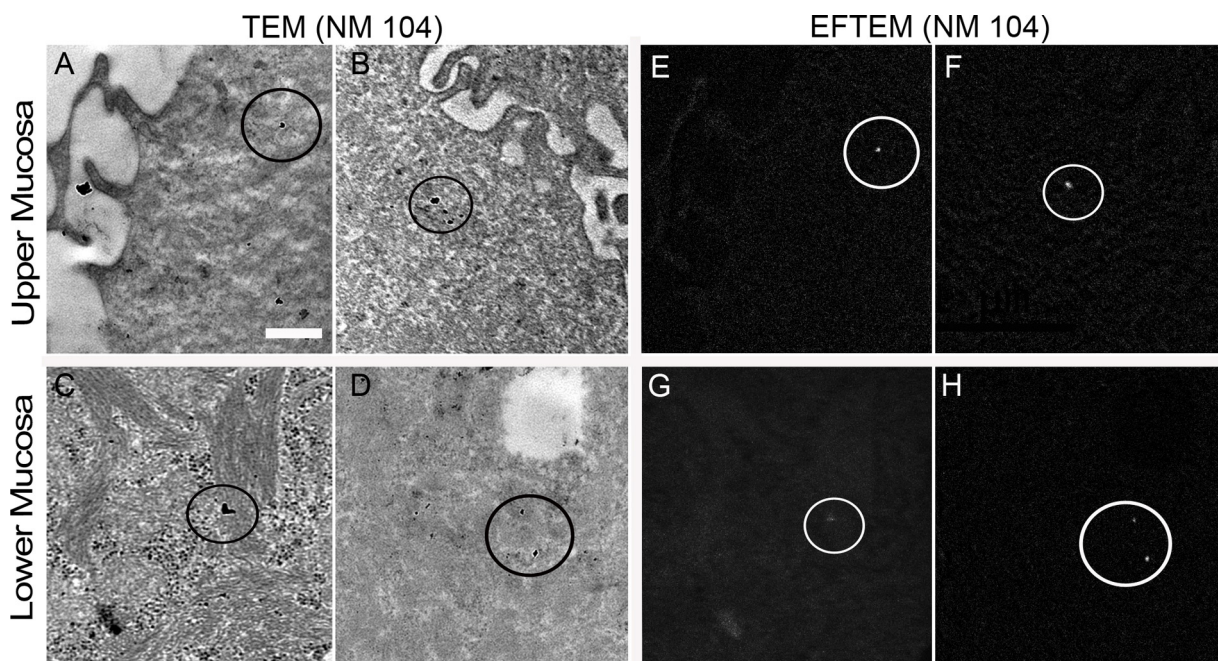


Fig. 2. TEM images of the buccal mucosa (cross sections) after 4 h particle incubation. NM 104 particles were found in the upper mucosa (superficial epithelium; upper panel) and in the lower mucosa (basal lamina/ connective tissue; lower panel). NM 104 particles were predominantly found non-membrane bound in the cytoplasm (A–D, circles). To verify the particles of interest, EFTEM was performed and elemental maps were made with a three-window method (E–H). The maps verified the element titanium (white spots). (Scale bar = 500 nm).

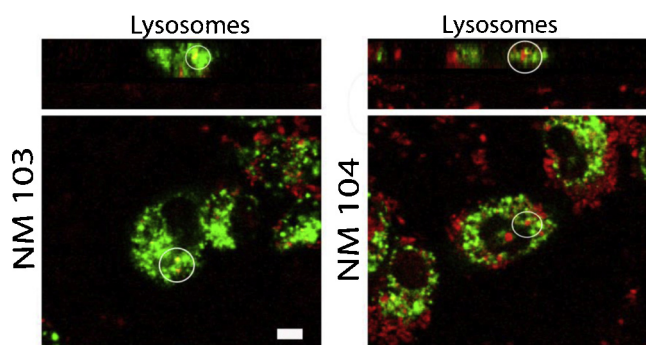


Fig. 3. Intracellular localization of fluorescently labeled TiO_2 particles conducted with LSM. The small panels show the virtual sections of the acquired z-stacks. Co-localization (yellow spots) of NM 103 particles (red) with lysosomes (green) occurred. NM 104 particles (red) were not detected within the lysosomes (green). The white circles indicate verified TiO_2 particles (scale bar = $20 \mu\text{m}$) (For interpretation of the references to color in this figure legend, the reader is referred to the web version of this article.).

not located within these acidic organelles supports the hypothesis of a further existing, probably passive uptake mechanism.

3.3. Cytotoxicity/ROS production/genotoxicity

Freely distributed NPs have the potential to interact with intracellular proteins, organelles and/or cell nuclei. Consequently, they may deposit in mitochondria, damage mitochondrial function and trigger the generation of ROS [45], resulting in long-term effects such as inflammation and/or impairment of the cell viability [46]. Particle localization of labeled TiO_2 NPs within mitochondria was studied using MitoTracker DeepRed 633. LSM images demonstrated

that neither hydrophobic NM 103 nor hydrophilic NM 104 lodged inside mitochondria (Fig. 4A). Although TiO_2 particles do not penetrate into mitochondria, a potential damaging effect cannot be excluded since particles may injure the outer mitochondrial membrane. Thus, additional screening assays were performed. The cell viability was measured by MTS assay. The results (Fig. 4B) indicated no cytotoxic effects of NM 103 and NM 104 within the tested concentration range (up to $200 \mu\text{g}/\text{mL}$). However, it is noticeable that in both cases the mitochondrial activity/viability was higher compared to the cellular control. The increase in metabolic activity can imply an indication of a cellular stress situation. To clarify this issue, the mitochondrial membrane-potential, mandatory for maintaining the physiological function of the cells, was examined [47]. A loss in the membrane-potential turns out in energy depletion and as a further consequence in cell death. The dye TMRM functions as a mitochondrial membrane potential sensor and was used to evaluate temporal changes. The fluorescence was quenched significantly to 93–85% for NM 103 particles and to 77–74% for NM 104 particles (Fig. 4C, $P < 0.05$). The unbalancing effect of the mitochondrial membrane potential was more pronounced for hydrophilic NM 104 particles than for the hydrophobic ones. This can be explained by the fact that NM 104 particles were not vesicular bound and, thus, able to interfere with the outer mitochondrial membrane. However, a reduced membrane-potential of mitochondria indicates the first sign of a programmed cell death. Changes in mitochondrial functions are followed by further cellular alterations that are important in modulating the apoptotic process, such as the production of ROS [48,49]. To evaluate the potential generation of ROS, the oxidation of DHE was measured in the absence of UV light. The data revealed that NM 103 caused a higher ROS production compared to the untreated cells (Fig. 5). However, the obtained relative fluorescence was markedly lower than the positive control (i.e., $200 \mu\text{M}$).

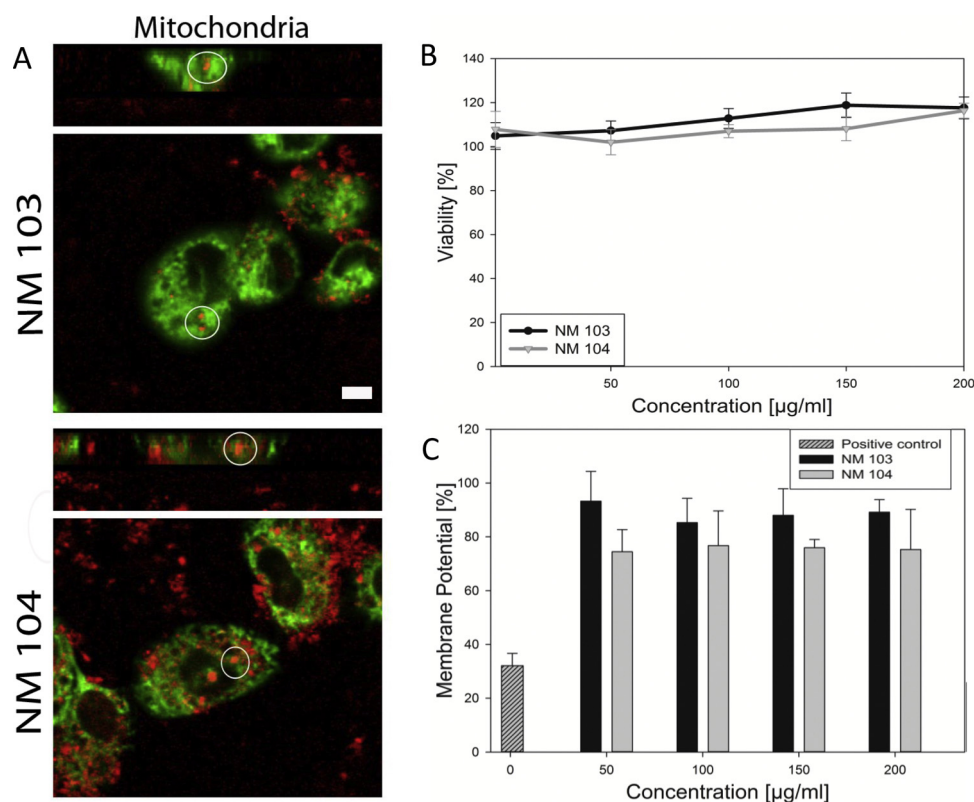


Fig. 4. (A) Intracellular localization of fluorescently labeled TiO_2 particles showed that neither 103 nor NM 104 particles (red) lodged in mitochondrial compartments (green). The white circles indicate verified TiO_2 particles (scale bar = $20 \mu\text{m}$). (B) The cell viability of buccal TR146 cells was evaluated after 4 h TiO_2 exposure using MTS assay and (C) temporal changes in mitochondrial membrane potential were determined using the dye TMRM. Untreated cells were set as negative control and H_2O_2 as positive control (For interpretation of the references to color in this figure legend, the reader is referred to the web version of this article.).

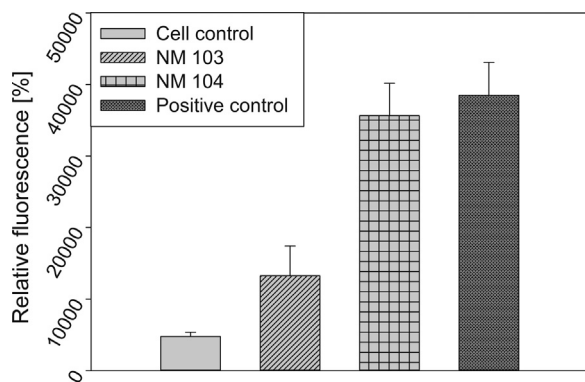


Fig. 5. Generation of ROS in TR146 cells was performed after 4 h TiO₂ exposure (100 µg/mL). Untreated cells were used as negative control, while H₂O₂ was set as positive control.

In contrast, NM 104 significantly triggered the generation of ROS. The degree of DHE oxidation was comparable with the positive control (200 µM H₂O₂).

These data strongly suggest that freely distributed hydrophilic TiO₂ particles in the cytoplasm have a stronger influence on cell homeostasis than hydrophobic particles, which are entrapped in endosomes/lysosomes. In addition, free NPs may enter the nucleus, interfere with the DNA and cause (in long term) gene mutation. To study induced point mutations in detail, a mutagenicity test (HPRT gene mutation assay) was performed. We found that neither NM 103 nor NM 104 triggered gene mutation in buccal epithelial cells (data not shown). No rise in mutant frequency was seen and the values were in the same range as cells treated with PBS.

4. Conclusions

Intrinsic particle characteristics, such as charge or hydrophilicity/hydrophobicity are known to contribute actively to the interactions between NPs and biological systems. The current study demonstrates that hydrophilic as well as hydrophobic TiO₂ NPs agglomerated under oral physiological conditions. Nevertheless, LD data demonstrated that 10% were still available in the nanosized range and penetrated the upper and lower buccal epithelium, independent on the hydrophilicity. However, differences were observed in the intracellular particle localization. Hydrophobic NM 103 particles were closely aligned to the cell membrane, wrapped up and most of them were found in endosomes/lysosomes. Toxic side effects were accordingly low since particles – separated from the cytoplasm – do not react with intracellular structures. In contrast, hydrophilic NM 104 particles directly entered the cells without affecting the membrane integrity and were found freely distributed in the cytoplasm. Although the viability of the buccal epithelial cells was neither affected by hydrophilic nor by hydrophobic TiO₂ particles, essential functions for cell homeostasis were impaired. Both materials showed a decrease of the mitochondrial membrane potential and provoked a sustained ROS level, which was significantly higher for hydrophilic NM 104 particles.

Acknowledgements

This work was supported by Land Steiermark and the European Commission (European funds for national development A3-11.N-14/2010-5). The authors want to thank Tatjana Kueznik, Claudia Meindl, Medical University of Graz for their assistance with LSM and Ramona Baumgartner, Nathalie Klackl and Carolin Tetyczka for their assistance with cytotoxicity assays. BioNanoNet GmbH is gratefully acknowledged.

References

- [1] R. Baan, K. Straif, Y. Grosse, B. Secretan, F. El Ghissassi, V. Coglianò, Carcinogenicity of carbon black, titanium dioxide, and talc, *Lancet Oncol.* 7 (2006) 295–296.
- [2] U.S.F.a.D. Administration, Listing of color additives exempt from certification in: Title 21 - Food and Drugs, Code of Federal Regulations 73.575, U.S., 1996.
- [3] E. Fröhlich, E. Roblegg, Models for oral uptake of nanoparticles in consumer products, *Toxicology* 291 (2012) 10–17.
- [4] P.W. Wertz, C.A. Squier, Cellular and molecular basis of barrier function in oral epithelium, *Crit. Rev. Ther. Drug Carrier Syst.* 8 (1991) 237–269.
- [5] E. Roblegg, E. Fröhlich, C. Meindl, B. Teubl, M. Zaversky, A. Zimmer, Evaluation of a physiological in vitro system to study the transport of nanoparticles through the buccal mucosa, *Nanotoxicology* 6 (2012) 399–413.
- [6] B.J. Teubl, C. Meindl, A. Eitzlmayr, A. Zimmer, E. Fröhlich, E. Roblegg, In-vitro permeability of neutral polystyrene particles via buccal mucosa, *Small* 9 (2012) 457–466.
- [7] B.J. Teubl, G. Leitinger, M. Schneider, C.-M. Lehr, E. Fröhlich, A. Zimmer, E. Roblegg, The buccal mucosa as a route for TiO₂ nanoparticle uptake, *Nanotoxicology* (2014) 1–9.
- [8] S.S. Watson, D. Beydoun, J.A. Scott, R. Amal, The effect of preparation method on the photoactivity of crystalline titanium dioxide particles, *Chem. Eng. J.* 95 (2003) 213–220.
- [9] L. Braydich-Stolle, N. Schaublin, R. Murdock, J. Jiang, P. Biswas, J. Schlager, S. Hussain, Crystal structure mediates mode of cell death in TiO₂ nanotoxicity, *J. Nanopart. Res.* 11 (2009) 1361–1374.
- [10] M.E. Carloti, E. Ugazio, S. Sapino, I. Fenoglio, G. Greco, B. Fubini, Role of particle coating in controlling skin damage photoinduced by titania nanoparticles, *Free Radical Res.* 43 (2009) 312–322.
- [11] V.P. Judin, The lighter side of TiO₂, *Chem. Braz.* 29 (1993) 503–506.
- [12] A.T. Florence, A.M. Hillery, N. Hussain, P.U. Jani, Nanoparticles as carriers for oral peptide absorption: studies on particle uptake and fate, *J. Control. Release* 36 (1995) 39–46.
- [13] R. Qiao, A.P. Roberts, A.S. Mount, S.J. Klaine, P.C. Ke, Translocation of c60 and its derivatives across a lipid bilayer, *Nano Lett.* 7 (2007) 614–619.
- [14] Y. Li, X. Chen, N. Gu, Computational investigation of interaction between nanoparticles and membranes: hydrophobic/hydrophilic effect, *J. Phys. Chem. B* 112 (2008) 16647–16653.
- [15] S. Hackenberg, G. Friehs, K. Froelich, C. Ginzkey, C. Koehler, A. Scherzed, M. Burghartz, R. Hagen, N. Kleinsasser, Intracellular distribution, geno- and cytotoxic effects of nanosized titanium dioxide particles in the anatase crystal phase on human nasal mucosa cells, *Toxicol. Lett.* 195 (2010) 9–14.
- [16] H.L. Karlsson, J. Gustafsson, P. Cronholm, L. Möller, Size-dependent toxicity of metal oxide particles – a comparison between nano- and micrometer size, *Toxicol. Lett.* 188 (2009) 112–118.
- [17] V.L. Bykov, [The tissue and cell defense mechanisms of the oral mucosa], *Morfologija* 110 (1996) 14–24.
- [18] J. Braun, Titanium dioxide – a review, *J. Coat. Technol.* 69 (1997) 59–72.
- [19] A. Weir, P. Westerhoff, L. Fabricius, K. Hristovski, N. von Goetz, Titanium dioxide nanoparticles in food and personal care products, *Environ. Sci. Technol.* 46 (2012) 2242–2250.
- [20] C.A. Lesch, C.A. Squier, A. Cruchley, D.M. Williams, P. Speight, The permeability of human oral mucosa and skin to water, *J. Dent. Res.* 68 (1989) 1345–1349.
- [21] J.R. Gurr, A.S. Wang, C.H. Chen, K.Y. Jan, Ultrafine titanium dioxide particles in the absence of photoactivation can induce oxidative damage to human bronchial epithelial cells, *Toxicology* 213 (2005) 66–73.
- [22] J.M. Veranth, E.G. Kaser, M.M. Veranth, M. Koch, G.S. Yost, Cytokine responses of human lung cells (BEAS-2B) treated with micron-sized and nanoparticles of metal oxides compared to soil dusts, part, *Fibre Toxicol.* 4 (2007) 2.
- [23] H.-W. Chen, S.-F. Su, C.-T. Chien, W.-H. Lin, S.-L. Yu, C.-C. Chou, J.J.W. Chen, P.-C. Yang, Titanium dioxide nanoparticles induce emphysema-like lung injury in mice, *FASEB J.* 20 (2006) 2393–2395.
- [24] C. De Haar, I. Hassing, M. Bol, R. Bleumink, R. Pieters, Ultrafine but not fine particulate matter causes airway inflammation and allergic airway sensitization to co-administered antigen in mice, *Clin. Exp. Allergy* 36 (2006) 1469–1479.
- [25] V.H. Grassian, T. O'Shaughnessy, A. Adamcakova-Dodd, J.M. Pettibone, P.S. Thorne, Inhalation exposure study of titanium dioxide nanoparticles with a primary particle size of 2 to 5 nm, *Environ. Health Perspect.* 115 (2007) 397–402.
- [26] G. Oberdörster, J. Ferin, B.E. Lehnert, Correlation between particle size, in vivo particle persistence, and lung injury, *Environ. Health Perspect.* 5 (1994) 173–179.
- [27] R. Shukla, V. Bansal, M. Chaudhary, A. Basu, R.R. Bhande, M. Sastry, Biocompatibility of gold nanoparticles and their endocytotic fate inside the cellular compartment: a microscopic overview, *Langmuir* 21 (2005) 10644–10654.
- [28] R.H. Müller, Surface Hydrophobicity-Determination by Rose Bengal (RB) Adsorption Methods, in: *Colloidal Carriers for Controlled Drug Delivery and Targeting*, CRC, Press, Stuttgart, 1991, pp. 99–109.
- [29] K.T. Thurn, T. Paunesku, A. Wu, E.M.B. Brown, B. Lai, S. Vogt, J. Maser, M. Aslam, V. Dravid, R. Bergan, G.E. Woloschak, Labeling TiO₂ nanoparticles with dyes for optical fluorescence microscopy and determination of TiO₂-DNA nanoconjugate stability, *Small* 5 (2009) 1318–1325.

- [30] J. Jacobsen, M. van Deurs, M.R. Rassing, TR146 cells grown on filters as a model for human buccal epithelium: I. Morphology, growth, barrier properties, and permeability, *Int. J. Pharm.* 125 (1995) 165–184.
- [31] H.M. Nielsen, M.R. Rassing, TR146 cells grown on filters as a model of human buccal epithelium: IV. Permeability of water, mannitol, testosterone and β^2 -adrenoceptor antagonists. Comparison to human, monkey and porcine buccal mucosa, *Int. J. Pharm.* 194 (2000) 155–167.
- [32] K. Buch, T. Peters, T. Nawroth, M. Sanger, H. Schmidberger, P. Langguth, Determination of cell survival after irradiation via clonogenic assay versus multiple MTT assay – a comparative study, *Radiat. Oncol.* 7 (2012) 1–6.
- [33] A.P. Zhang, Y.P. Sun, Photocatalytic killing effect of TiO₂ nanoparticles on Ls-174-t human colon carcinoma cells, *World J. Gastroenterol.* 10 (2004) 3191–3193.
- [34] J. Dekker, J.W.A. Rossen, H.A. Buller, A.W.C. Einerhand, The MUC family: an obituary, *Trends Biochem. Sci.* 27 (2002) 126–131.
- [35] D.J. Thornton, I. Carlstedt, M. Howard, P.L. Devine, M.R. Price, J.K. Sheehan, Respiratory mucins: identification of core proteins and glycoforms, *Biochem. J.* 316 (1996) 967–975.
- [36] B.J. Van Klinken, J. Dekker, H.A. Buller, A.W. Einerhand, Mucin gene structure and expression: protection vs. adhesion, *J. Am. Physiol. Gastrointest. Liver Physiol.* 269 (1995) G613–G627.
- [37] C.M. Lehr, From sticky stuff to sweet receptors – achievements, limits and novel approaches to bioadhesion, *Eur. J. Drug Metab. Pharmacokinet.* 21 (1996) 139–148.
- [38] T. Jung, W. Kamm, A. Breitenbach, E. Kaiserling, J.X. Xiao, T. Kissel, Biodegradable nanoparticles for oral delivery of peptides: is there a role for polymers to affect mucosal uptake? *Eur. J. Pharm. Biopharm.* 50 (2000) 147–160.
- [39] E. Frohlich, C. Meindl, E. Roblegg, B. Ebner, M. Absenger, T. Pieber, Action of polystyrene nanoparticles of different sizes on lysosomal function and integrity part, *Fibre Toxicol.* 9 (2012) 26.
- [40] M. Geiser, B. Rothen-Rutishauser, N. Kapp, S. Schurch, W. Kreyling, H. Schulz, M. Semmler, V. Im Hof, J. Heyder, P. Gehr, Ultrafine particles cross cellular membranes by nonphagocytic mechanisms in lungs and in cultured cells, *Environ. Health Perspect.* 113 (2005) 1555–1560.
- [41] A. Verma, O. Uzun, Y. Hu, Y. Hu, H.-S. Han, N. Watson, S. Chen, D.J. Irvine, F. Stellacci, Surface-structure-regulated cell-membrane penetration by monolayer-protected nanoparticles, *Nat. Mater.* 7 (2008) 588–595.
- [42] P.R. Leroueil, S. Hong, A. Mecke, J.R. Baker, B.G. Orr, M.M. Banaszak Holl, Nanoparticle Interaction with Biological Membranes: Does Nanotechnology Present a Janus Face?, *Acc. Chem. Res.* 40 (2007) 335–342.
- [43] S. Singh, T. Shi, R. Duffin, C. Albrecht, D. van Berlo, D. Hohr, B. Fubini, G. Martra, I. Fenoglio, P.J.A. Borm, R.P.F. Schins, Endocytosis, oxidative stress and IL-8 expression in human lung epithelial cells upon treatment with fine and ultrafine TiO₂: Role of the specific surface area and of surface methylation of the particles, *Toxicol. Appl. Pharmacol.* 222 (2007) 141–151.
- [44] R.C. Stearns, J.D. Paulauskis, J.J. Godleski, Endocytosis of ultrafine particles by A549 cells, *Am. J. Respir. Cell Mol. Biol.* 24 (2001) 108–115.
- [45] J.E. Kokoszka, P. Coskun, L.A. Esposito, D.C. Wallace, Increased mitochondrial oxidative stress in the Sod2 (+/–) mouse results in the age-related decline of mitochondrial function culminating in increased apoptosis, *Proc. Natl. Acad. Sci. U. S. A.* 98 (2001) 2278–2283.
- [46] A. Nel, T. Xia, L. Madler, N. Li, Toxic potential of materials at the nanolevel, *Science* 311 (2006) 622–627.
- [47] F.V. Pallardo, A. Lloret, M. Lebel, M. d’Ischia, V.C. Cogger, D.G. Le Couteur, M.N. Gadaleta, G. Castello, G. Pagano, Mitochondrial dysfunction in some oxidative stress-related genetic diseases: ataxia-telangiectasia, down syndrome, Fanconi anaemia and Werner syndrome, *Biogerontology* 11 (2010) 401–419.
- [48] D.R. Green, J.C. Reed, Mitochondria and apoptosis, *Science* 281 (1998) 1309–1312.
- [49] G. Kroemer, B. Dallaporta, M. Resche-Rigon, The mitochondrial death/life regulator in apoptosis and necrosis, *Annu. Rev. Physiol.* 60 (1998) 619–642.